Anomalous Electronic State in $CaCrO_3$ and $SrCrO_3$

J.-S. Zhou,[1] C.-Q. Jin,[2] Y.-W. Long,[2] L.-X. Yang,[2] and J. B. Goodenough[1]

[1]*Texas Materials Institute, University of Texas, 1 University Station, C2201, Austin, Texas 78712, USA*

[2]*Institute of Physics, Chinese Academy of Science, P.O. Box 603, Beijing, China*

(Received 23 December 2004; published 2 February 2006)

Comprehensive measurements of electrical transport properties under pressure, thermal conductivity, magnetic susceptibility, and room-temperature compressibility have been used to characterize $SrCrO_3$ and $CaCrO_3$ perovskites synthesized under high pressure. Comparison with other narrow-band perovskite oxides suggests that their anomalous physical properties are correlated with bond-length instabilities caused by the crossover from localized to itinerant electronic behavior.

DOI: 10.1103/PhysRevLett.96.046408 PACS numbers: 71.27.+a, 64.30.+t, 71.28.+d, 71.30.+h

First-row transition-metal oxides with the perovskite or a perovskite-related structure allow a study of the transition from localized to itinerant electronic behavior in states of $3d$-orbital parentage by isovalent or heterovalent substitution of the large A cation. Complete crossover has been monitored in the mixed-valent $La_{2-x}Sr_xCuO_4$ superconductive system and the $La_{1-x}(Ca, Sr)_xMnO_3$ system exhibiting a colossal magnetoresistance. Access to the electronic state at crossover in a single-valent system, however, is always plagued by structural instabilities. High pressure has proven to be very useful, and critical in some cases, for studying physical properties in the narrow-band perovskites exhibiting structural instabilities. The $RNiO_3$ family is now a well-studied system showing the complete evolution from a paramagnetic metal to a magnetic insulator [1]. The insulator phase below an insulator-metal transition temperature T_{IM} does not have globally ionic Ni-O bonding; this bonding segregates into ordered ionic and covalent bonds. It is important to note that the difference between the more ionic Ni-O bond and the more covalent Ni-O bond decreases with increasing size of the rare-earth ion [1,2]. Therefore, it becomes increasingly difficult to resolve the difference between these two kinds of Ni-O bond, and an intermediate Ni-O bond length is stabilized as the itinerant electronic state is approached. $SrCrO_3$ and $CaCrO_3$ offer the opportunity to study the structural and physical properties in a phase having a Cr-O bond length other than its regular ionic bond length given in the literature. Moreover, comparison between the $ACr^{4+}O_3$ and the $RNiO_3$ family can reveal the difference between π-bonding electrons and the σ-bonding electrons at the crossover. The $ACr^{4+}O_3$ compounds were initially studied some three decades ago [3–5]. These preliminary studies reported a $T_N \approx 90$ K in antiferromagnetic $CaCrO_3$ and no long-range magnetic order in $SrCrO_3$. Further study of these materials has been inhibited by the need to prepare them under high oxygen pressure. In this Letter, we report a comprehensive characterization of $SrCrO_3$ and $CaCrO_3$ polycrystalline samples synthesized under high pressure by resolving the crystal structure and by measuring electrical transport properties, thermal conductivity, magnetic susceptibility, and the equation of state (EOS). We demonstrate remarkable bonding instabilities in these compounds by their glassy thermal conductivity, pressure-induced bond softening, and insulator-metal transition.

High-pressure synthesis was carried out as described previously [4] except that commercial high-purity (3N) CaO, SrO, and CrO_2 were used as the starting materials. As-made pellets of high-pressure products include about 5% impurity phases as initially checked by powder x-ray diffraction. Powder samples of the high-purity perovskite phase, as shown by the x-ray powder diffraction in Fig. 1, can be obtained by washing the high-pressure sample with dilute acid. The high-purity powder was pressed into a pellet for the magnetic measurements whereas as-made pellets of the high-pressure products were cut with a diamond saw into rectangular bars for the transport measurements. X-ray diffraction data were collected with 0.02° and 15 s/step. Diffraction data were refined with the cubic $Pm3m$ space group in $SrCrO_3$ and the orthorhombic $Pbnm$ in $CaCrO_3$ by using Rietveld analysis (Fullprof program) [6]; the analysis gives lattice parameters $a = 3.81982(3)$ Å for $SrCrO_3$ and $a = 5.2886(1)$ Å, $b = 5.3172(2)$ Å, and $c = 7.4844(1)$ Å for $CaCrO_3$. Other relevant structural parameters are listed inside Fig. 1. These lattice parameters match those in the literature [3–5] to the third decimal place. The comparisons of lattice parameters and the Seebeck coefficient with that from Ref. [5] confirm that we have precisely the same compounds as the samples made before in which the oxygen stoichiometry was determined chemically [3,4]. Moreover, the occupied density from the Rietveld analysis also indicates that the compounds are close to chemical stoichiometry. The magnetization measurements were performed on a SQUID magnetometer (Quantum Design), and all other measurements of transport properties were carried out on homemade setups. The x-ray diffraction under high pressure was carried out on a diamond-anvil cell (DAC) as described previously [7]. A small amount of CaF_2 powder was mixed with the sample as the pressure manometer [8]. The measurement of resistance under pressure was also made in a DAC with MgO as the pressure medium.

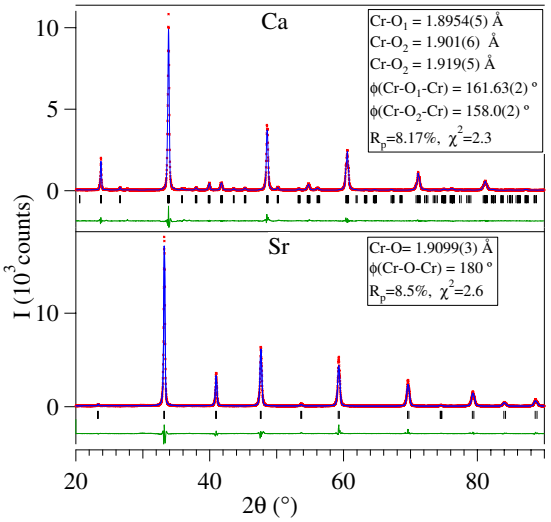

FIG. 1 (color online). X-ray powder diffraction pattern for $SrCrO_3$ and $CaCrO_3$ with Cu $K\alpha$ radiation. Fitting patterns from the Rietveld analysis are also superimposed in the figure. Results from the Rietveld analysis are listed inside the figure.

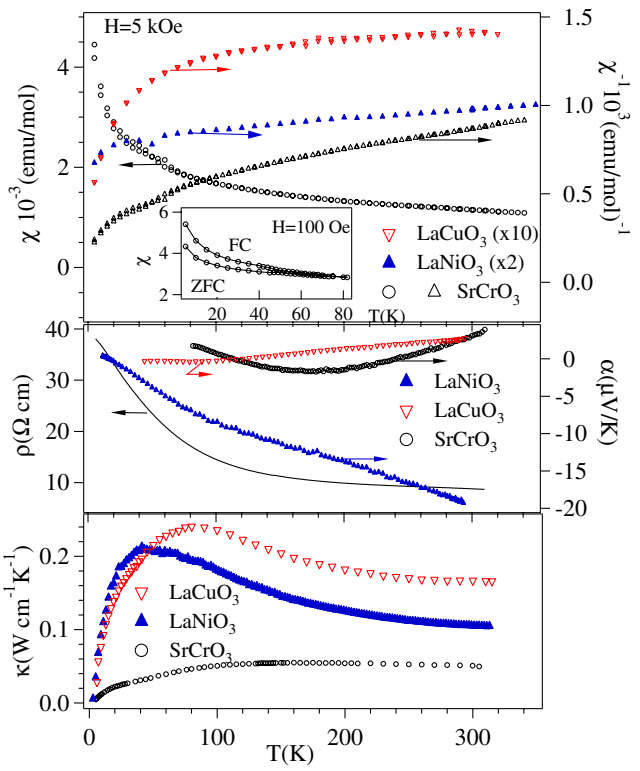

FIG. 2 (color online). Temperature dependences of the magnetization, resistivity, thermoelectric power, and thermal conductivity of $SrCrO_3$, $LaNiO_3$, and $LaCuO_3$.

Although the inverse magnetic susceptibility $\chi^{-1}(T)$ of $SrCrO_3$ in Fig. 2(a) shows a quite remarkable temperature dependence, fitting to the Curie-Weiss law gives a $\mu_{\text{eff}} \approx 8.3\mu_B$, which is significantly higher than the expected value for two localized t_2 electrons on a Cr^{4+} ion. Such a failure of the Curie-Weiss law is typical of a nonlocalized electronic state in $SrCrO_3$. On the other hand, in comparison with other strongly correlated metallic perovskites such as $LaNiO_3$ and $LaCuO_3$, the magnitude of $\chi(300\ \text{K})$ is nearly double that of $LaNiO_3$ and an order of magnitude higher than that of $LaCuO_3$. Moreover, the $\chi^{-1}(T)$ curves of $LaNiO_3$ and $LaCuO_3$, shown in Fig. 2(a), are much less temperature dependent than the $\chi^{-1}(T)$ of $SrCrO_3$. This finding shows the presence of a considerable volume fraction of strong-correlation fluctuations [9] in $SrCrO_3$. Measurement in 100 Oe, plotted in the inset of Fig. 2(a), shows a clear separation between the field-cooled (FC) and zero-field-cooled (ZFC) susceptibility of $SrCrO_3$, which may signal the existence of some short-range ordering although no T_N is discernible. The weak temperature dependence and semiconductorlike $\rho(T)$, solid line of Fig. 2(b), may represent either grain-boundary scattering in this polycrystalline sample or an exotic electronic conduction. The very small Seebeck coefficient α, which is related to the bulk property, indicates a high carrier density. However, the $\alpha(T)$ curve of $SrCrO_3$ does not behave like that of a metal as was found in $LaNiO_3$ (n-type) and $LaCuO_3$ (p-type). A minimum of $\alpha(T)$ occurring near 160 K is at too high a temperature for the phonon-drag effect; this temperature corresponds roughly to the deviation from a linear relationship in $\chi^{-1}(T)$ and the onset temperature where the thermal conductivity $\kappa(T)$ of Fig. 2(c) starts to decrease. The glassy $\kappa(T)$ of $SrCrO_3$ is in sharp contrast to the thermal conductivity found in the other strongly correlated metals $LaNiO_3$ and $LaCuO_3$. The electronic conduction contributes to the heat transfer in these metallic compounds. The phononlike $\kappa(T)$ of the lattice contribution can be derived by using the electrical conductivity via the Wiedemann-Franz law [10]. Up to this point, $SrCrO_3$ behaves like neither a paramagnetic metal nor a magnetic insulator. A reduced and glassy $\kappa(T)$ signals some remarkable bond-length fluctuations.

The $\chi^{-1}(T)$ of $CaCrO_3$ in Fig. 3(a) shows a much steeper temperature dependence than $SrCrO_3$. A $\mu_{\text{eff}} \approx 3.7\ \mu_B$ obtained by fitting $\chi^{-1}(T)$ to the Curie-Weiss law is not too far from the localized-electron spin-only value. The magnetic transition at $T_N \approx 90$ K also matches that reported previously [4]. However, not observed in the early experiments is a large splitting of the ZFC and FC $\chi(T)$ curves. The extremely small and nonlinear magnetization $M(H)$ are indicative of a canted spin structure below T_N and a large magnetocrystalline anisotropy. However, a drop of $\kappa(T)$ in Fig. 3(b) on cooling below $T_N \approx 90$ K is opposite to what happens in most magnetic insulators and in the hexagonal $RMnO_3$ compounds where the phonons are restored below T_N [11]. The overall suppression of $\kappa(T)$ in $CaCrO_3$ appears to be related to bond-length fluctuations that are not associated with spin fluctuations. Moreover, short-range magnetic order must induce some orbital fluctuations at temperatures well above 90 K in order to account for a gradual decline of $\kappa(T)$ with decreasing

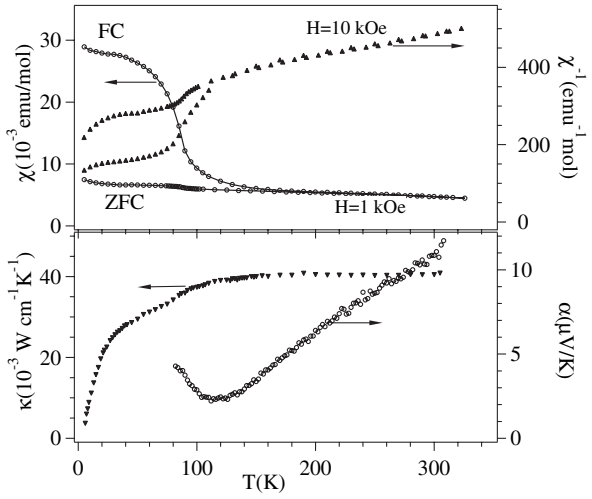

FIG. 3. The same as Fig. 2 (without resistivity) for $CaCrO_3$. Inset: magnetization to 5.5 T at 5 K.

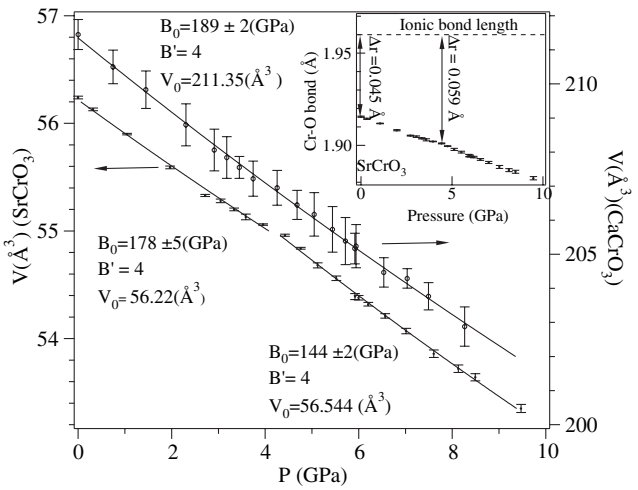

FIG. 4. Pressure dependence of the volume for $SrCrO_3$ and $CaCrO_3$. Inset: the pressure dependence of the Cr-O bond length for $SrCrO_3$; see the text for details.

temperature below 160 K where the FC and ZFC $\chi(T)$ curves diverge above T_N.

A physically sound solution to these anomalous physical properties must rely on the study of their crystal structure. The structure simulation obtained by using the software SPUDS [12] provides a guideline to the structure with ionic bonds [13]. Results from the Rietveld analysis as listed in Fig. 1 show a significantly shorter Cr-O bond length by a $\Delta r \approx 0.05$ Å in both $CaCrO_3$ and $SrCrO_3$ than the ionic Cr-O bond length 1.96 Å calculated by SPUDS. A nearly identical bond-length reduction $\Delta r \approx 0.042$ Å from the ionic bond to the intermediate Ni-O bonding state at the crossover from localized to itinerant electronic behavior has been seen in $RNiO_3$ [1]. On the other hand, a further reduction by a $\Delta r \geq 0.06$ Å from the ionic Ni-O bond length is needed in order for $RNiO_3$ to be metallic. Comparison with the $RNiO_3$ family motivates structural studies under chemical and hydrostatic pressure. We have chosen to study $SrCrO_3$ and $CaCrO_3$ under pressure. Fitting the V-P curve of Fig. 4 to the Birch-Murnaghan equation gives a bulk modulus $B_0 = 178 \pm 5$ GPa for $P <$ 4 GPa, which falls in line with the B_0 for a broad range of $A^{2+}B^{4+}O_3$ perovskite oxides [14]. At $P > 4$ GPa, $SrCrO_3$ remains a cubic perovskite, but the structure becomes much more compressible by showing a much reduced $B_0 = 144 \pm 2$ GPa. A similarly low bulk modulus in perovskite oxides has only been seen in two other cases so far: (a) $B_0 = 122$–150 GPa for $LaCoO_3$ where pressure induces a spin-state transition [15,16] and (b) $B_0 =$ 144 GPa for $Nd_{0.5}Sm_{0.5}NiO_3$ where pressure induces a transition from an insulator to a metallic phase [7]. Both cases show that the perovskite becomes much more compressible where a pressure-induced electronic-state transition is involved. Interestingly, the inset of Fig. 4 shows that $SrCrO_3$ becomes "soft" where the difference between the ionic Cr-O bond from SPUDS and the Cr-O bond under pressure reaches a $\Delta r \approx 0.059$ Å, which matches almost perfectly to the bond-length reduction from the ionic to the metallic bond in $RNiO_3$. In order to confirm the origin of the bond softening near 4 GPa, we have performed the measurement of resistance under pressure to 24 GPa shown in Fig. 5. In this ln$R$ versus P plot, it is clear that R changes against P more dramatically at low pressure than at higher pressures. This change, however, is still not solid proof for an electronic-state transition to a metallic phase near 4 GPa since grain-boundary resistance is also lowered dramatically at relatively low pressures. As plotted in the inset of Fig. 5, metallic conductivity becomes clearly visible at 10 GPa. The insulator-metal transition temperature T_{IM} where $R(T)$ shows a minimum, decreases under even higher pressure. It requires a measurement of $R(T)$ at $T >$ 300 K in order to locate precisely this shallow minimum of $R(T)$ where T_{IM} is near room temperature. However, extrapolation of the $T_{IM}(P)$ curve to lower pressure, see inset of Fig. 5, would locate a $T_{IM} \approx 300$ K near 5 GPa. This result not only confirms that the bond softening near 4 GPa found in the structural study under pressure is due to the electronic transition to a metallic phase, but it also proves unambiguously that $SrCrO_3$ is a paramagnetic insulator with bond-length instabilities at ambient pressure.

Results of Rietveld analysis provide important additional structural features for characterizing the bonding in $SrCrO_3$ and $CaCrO_3$:

(1) A stretched Cr-O bond in $SrCrO_3$.—A tolerance factor $t < 1$ in a perovskite AMO_3 places the A-O bond under tensile stress and the M-O bond under a compressive stress. This mismatch is released by a cooperative octahedral-site rotation, and the M-O bond length remains nearly a constant for $t < 1$ as long as there is no electronic transition [1]. However, the perovskite structure finds no way to relieve an M-O bond under tension for $t > 1$. The M-O bond length in the metastable high-pressure phase is

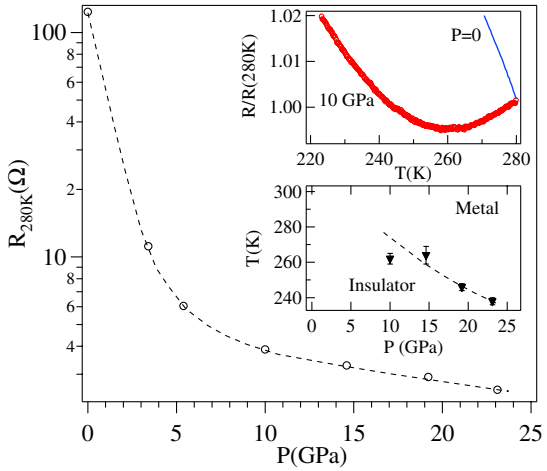

FIG. 5 (color online). Pressure dependence of the resistance at 280 K. Inset (a) temperature dependence of the renormalized resistance at different pressures; inset (b) pressure dependence of the metal-insulator transition temperature.

stretched due to the compressive stress on the too long equilibrium A-O bond length. As listed inside Fig. 1, the average bond length $\langle$Cr-O$\rangle = 1.905$ Å in $CaCrO_3$ is slightly smaller than the $\langle$Cr-O$\rangle = 1.9099$ Å in $SrCrO_3$, which suggests that the Cr-O bond in $SrCrO_3$ is stretched due to a tolerance factor $t > 1$.

(2) Sensitivity of the electronic bandwidth to the Cr-O-Cr bond angle.—The bandwidth W in the perovskite structure can be calculated for σ-bonding electrons via the formula [17] $W \approx \cos[(180° - \phi)/2]/d_{\text{Cr-O}}{}^{3.5}$. By using the structural parameters listed inside of Fig. 1, we obtained a $W = 0.10386$ (arb. unit) for $SrCrO_3$ versus $W = 0.10306$ for $CaCrO_3$. This tiny difference in the calculated bandwidth is insufficient to justify the transition from the paramagnetic, insulating phase of $SrCrO_3$ to the antiferromagnetic insulating phase of $CaCrO_3$. Some other factor such as the competition for the O:$2p_\pi$ electron between the A-O bond and Cr-O bonds should be taken into account.

(3) A Jahn-Teller distortion of the Cr^{4+}*-ion site.*—Cr^{4+}:$t_2{}^2$ is a Jahn-Teller ion like the V^{3+} ion. The J-T distortion is suppressed in the cubic $SrCrO_3$. In $CaCrO_3$, however, the Rietveld analysis gives three different Cr-O bond lengths. The difference between the longest and the shortest Cr-O bond is comparable to that found in YVO_3 at room temperature. Although the bond length splitting in a $MO_{6/2}$ octahedron depends on the octahedral rotation angle in the orthorhombic perovskites [18], the relatively large bond length splitting at 160° rotation angle in $CaCrO_3$ suggests that the J-T distortion may take place for the intermediate bond length between the typical ionic bond length and the metallic bond length.

In conclusion, the perovskite insulators $SrCrO_3$ and $CaCrO_3$ provide a unique example of the approach to crossover from localized to itinerant electronic behavior from the localized-electron side as the lattice instabilities do not manifest themselves as a phase segregation. We have demonstrated that the Cr-O bond length in these compounds is different from the ionic bond on the one side and a covalent (or metallic) bond on the other. The bonding instability in this phase leads to a significant degree of bond-length fluctuations that suppress the phonon thermal conductivity and are responsible for anomalous transport and magnetic properties. The bonding instability has been further confirmed by the pressure-induced bond softening where the electronic transition to the metallic phase takes place in $SrCrO_3$. Replacing Sr by Ca gives a negligible change of the bandwidth, but it may induce the J-T distortion of the Cr^{4+} sites in $CaCrO_3$. Narrowing of the π^* bandwidth appears to be dominated by a greater competition for the O-$2p_\pi$ electrons between the Ca-O bond versus Cr-O bond.

The NSF (Grants No. DMR0353362, No. DMR0132282), the Robert A. Welch Foundation, and NSFC (Grants No. 50328102, No. 50332020, No. 50321101) are thanked for financial support.

[1] J.-S. Zhou and J. B. Goodenough, Phys. Rev. B **69**, 153105 (2004).
[2] U. Staub *et al.*, Phys. Rev. Lett. **88**, 126402 (2002).
[3] B. L. Chamberland, Solid State Commun. **5**, 663 (1967).
[4] J. B. Goodenough, J. M. Longo, and J. A. Kafalas, Mater. Res. Bull. **3**, 471 (1968).
[5] J. F. Weiher, B. L. Chamberland, and J. L. Gillson, J. Solid State Chem. **3**, 529 (1971).
[6] J. Rodriguez-Carvajal, Physica (Amsterdam) **192B**, 55 (1993).
[7] J.-S. Zhou, J. B. Goodenough, and B. Dabrowski, Phys. Rev. B **70**, 081102 (2004).
[8] R. J. Angel, J. Phys. Condens. Matter **5**, L141 (1993).
[9] J.-S. Zhou and J. B. Goodenough, Phys. Rev. B **61**, 3196 (2000).
[10] J.-S. Zhou, J. B. Goodenough, and B. Dabrowski, Phys. Rev. B **67**, 020404 (2003).
[11] P. A. Sharma, J. S. Ahn, N. Hur, S. Park, S. B. Kim, S. Lee, J.-G. Park, S. Guha, and S.-W. Cheong, Phys. Rev. Lett. **93**, 177202 (2004).
[12] M. W. Lufaso and P. M. Woodward, Acta Crystallogr. Sect. B **57**, 725 (2001).
[13] J.-S. Zhou and J. B. Goodenough, Phys. Rev. Lett. **94**, 065501 (2005).
[14] N. L. Ross and R. J. Angel, Am. Mineral. **84**, 277 (1999).
[15] J.-S. Zhou, J.-Q. Yan, and J. B. Goodenough, Phys. Rev. B **71**, 220103(R) (2005).
[16] T. Vogt, J. A. Hriljac, N. C. Hyatt, and P. Woodward, Phys. Rev. B **67**, 140401 (2003).
[17] M. Medarde, J. Mesot, P. Lacorre, S. Rosenkranz, P. Fischer, and K. Gobreeht, Phys. Rev. B **52**, 9248 (1995).
[18] M. Marezio, J. P. Remeika, and P. D. Dernier, Acta Crystallogr. Sect. B **26**, 2008 (1970).